

Article

A Carbon Black/Polyvinyl Alcohol-Based Composite Thin Film Sensor Integrating Strain and Humidity Sensing Using the Droplet Deposition Method

Yiqun Zhang ^{1,2,†}, Xiaoyu Liu ^{1,†}, Xiaodong Wu ¹ , Qi Liu ^{1,2} and Zhuqing Wang ^{1,2,*}¹ School of Mechanical Engineering, Sichuan University, Chengdu 610065, China² Med+X Center for Manufacturing, West China Hospital of Sichuan University, Chengdu 610041, China

* Correspondence: wzhuqing@scu.edu.cn; Tel.: +86-13841149371

† These authors contributed equally to this work.

Abstract: Carbon black (CB) is a low-cost and excellent conductive material, and polyvinyl alcohol (PVA) is a non-conductive material with the advantages of easy processing and high mechanical stability. Here, we report a CB/PVA-based flexible conductive polymer film suitable for small strain detection and humidity detection. Thin film is formed by depositing the CB/PVA dispersion liquid droplets on a cleaned silicon/silicon dioxide (Si/SiO₂) substrate. Theoretically, CB/PVA films can be transferred or formed on other substrates, such as polydimethylsiloxane, which have the advantage of flexibility. The droplet deposition method not only enhances the controllability of the film thickness and wastage of materials, but also improves the sensitivity of the prepared film. The electrical conductivity of the CB/PVA composite film and the relationship between the resistance change and strain were measured by the four-point bending method, which showed a good gauge factor of 30 when the strain rate was 0.007%. In addition, the sensor also showed excellent sensing performance and repeatability at humidity levels ranging from 10% to 70% RH. These results demonstrate that the CB/PVA thin film prepared in this work has the advantages of a simple fabrication process, low-cost, multifunctional properties, and high device sensitivity, providing further insights for detecting minor strain and humidity.

Keywords: carbon black; droplet deposition; four-point bending; strain sensor; humidity sensor



Citation: Zhang, Y.; Liu, X.; Wu, X.; Liu, Q.; Wang, Z. A Carbon Black/Polyvinyl Alcohol-Based Composite Thin Film Sensor Integrating Strain and Humidity Sensing Using the Droplet Deposition Method. *Crystals* **2022**, *12*, 1316. <https://doi.org/10.3390/cryst12091316>

Academic Editors: Abdullah Mohamed Asiri and Helmut Cölfen

Received: 24 August 2022

Accepted: 15 September 2022

Published: 18 September 2022

Publisher's Note: MDPI stays neutral with regard to jurisdictional claims in published maps and institutional affiliations.



Copyright: © 2022 by the authors. Licensee MDPI, Basel, Switzerland. This article is an open access article distributed under the terms and conditions of the Creative Commons Attribution (CC BY) license (<https://creativecommons.org/licenses/by/4.0/>).

1. Introduction

In recent years, the rapid development of smart health detection equipment has been changing the traditional medical diagnosis mode and promoting the emergence of personal health management [1]. At the same time, people pay more and more attention to the real-time monitoring of their own physiological indicators and environmental conditions [2]. In particular, strain sensors and humidity sensors are almost essential parts of medical devices, since many human activities generate changes in pressure, such as a pulse (its pressure range is 0.2–3 kPa [3], which belongs to the micro pressure category), and environments that are too dry or too humid affect human health. Most traditional sensors are made of metal foils, ceramics, and semiconductors. However, these materials are inflexible, expensive, and difficult to fabricate when used for micro-sensors [4,5]. Therefore, more adoptable ways to fabricate strain and humidity sensors using both conductive fillers and non-conductive polymers have emerged [6–8]. Due to its outstanding electrical conductivity and excellent mechanical stability, carbonaceous material is often used as conductive filler for developing sensors [9]. For micro-electro-mechanical systems (MEMS), graphene, carbon nanotubes, and carbon black have been widely used as active layers [10–12]. In particular, the sensors made by carbon nanotubes have good flexibility but low sensitivity [13–15]. It has also been reported that the strain sensors made using graphene have good flexibility and sensitivity [16–20]. However, in terms of manufacturing costs, carbon nanotubes and

graphene are not good choices. On the contrary, carbon black is often selected due to its good electrical conductivity and low manufacturing cost [21,22]. Polyvinyl alcohol (PVA) has been widely used as a polymer matrix to fabricate flexible sensors due to its advantages of easy processing, durability, low cost, and nontoxicity [23]. Notably, PVA has the property of hydrophilic swelling. Therefore, sensors fabricated with PVA as the matrix material exhibit high sensitivity to humidity [24–27]. However, even with the same material, it is common for sensors to exhibit different electrical and mechanical properties under different fabrication methods.

Layers of material with thicknesses ranging from a few nanometers to several micrometers are called thin films [28]. It is noteworthy that for fabricating thin film sensors, the selection of both material and method of film formation plays an important role. The film formation method determines mostly the film uniformity, flatness, and thickness of the film, which are closely related to the performance of the sensor. There are many film-forming methods, such as spraying (the thickness of the prepared films is in the range of 1–500 μm), rod-coating (the thickness of the prepared film is more than 2 μm), drop-casting (the thickness of the prepared films is in the range of 5–500 μm), and spin coating (the thickness of the prepared films is in the range of 0–100 μm), available to prepare a thin conductive film [29,30]. In the spray coating method, the conductive dispersion is placed in a spray gun. Then it compresses air to atomize the dispersion into small droplets, which are deposited on the preheated substrate under the action of the airflow [15,31]. For the Meyer rods-coating method, the conductive dispersion ink is placed on the substrate, and then the Mayer rod is rolled at a certain speed to disperse the ink to form a uniform conductive film [32]. The drop-casting method is used to fabricate the film by dropping the dispersive liquid directly onto the substrate [33]. In the spin-coating method, the substrate is usually rotated on a high-speed rotating turntable. Owing to the high centrifugal force during spinning, the dispersed ink placed on the substrate spreads over the entire substrate area to form a thin film [34]. Both spin coating and spraying methods are efficient, but they waste material. The Meyer rod-coating method is suitable for mass production. However, it requires high viscosity and a large surface tension of the dispersion. The drop-casting method is low in cost, but it limits the uniformity of the film, and the thickness of prepared film is much thicker than that prepared by other methods. To overcome these limitations, a novel method is introduced to form highly controllable ultrathin films by using droplet-assisted deposition, which is a simple and efficient technique for preparing thin film sensors in the future.

Ke et al. showed a highly capacitive pressure sensors based on TPU/GNP/CNS composites with a high capacitive sensitivity of $2.05 \pm 0.13 \text{ MPa}^{-1}$ for a stress range of 0.1–1.3 MPa [35]. However, compared with piezoresistive sensors, capacitive sensors have parasitic capacitance, which may not only affect the sensitivity of capacitive sensors, but also cause interference to the sensor and affect its stability. Liu et al. reported a degradable strain sensor with a gauge factor of 4.3 using a paper substrate dipped into the aqueous suspension of carbon black (CB) and carboxymethyl cellulose (CMC) [36]. However, such paper-based sensors are prone to crack in the strain process and tended to lose most of their mechanical strength under wet conditions, which affects performance of the device. Though, Li et al. fabricated a strain sensor with the working range of 50~500% with the combinations of carbon black and silicone rubber using the drop-casting method, it revealed a maximum gauge factor of nearly 3.37 [37]. These works are basically aimed at the situation of relatively large strain, which is only suitable for elbow bending and posture monitoring, etc. Moreover, owing to the lower gauge factor value, such types of sensors are not suitable for use in situations where there is only a micro strain, such as pulse detection. Furthermore, they are all single-function strain sensors, which still have the potential to be improved into multifunctional sensors in complex environments.

In this paper, we proposed a piezoresistive CB/PVA composite film for micro strain and gas detection. From a materials perspective, on the one hand, the CB offers excellent merits such as good device performance and low manufacturing cost as a conductive filler for composite film. On the other hand, the PVA as non-conductive material has potential

benefits of easy film-forming ability and high mechanical properties. Furthermore, from the fabrication method point of view, this is a novel, simple, and low-cost method, which is not only applicable for fabricating strain sensors but is also suitable for fabricating many other thin-film sensors. The droplet deposition method used in this work showed great potential in reducing the wastage of the materials with high quality of the film. At room temperature and constant humidity, the four-point bending study was used to evaluate the sensing performance of the fabricated strain sensor, which showed a high sensitivity at a small strain ($GF \approx 30$). Furthermore, the sensor also showed an excellent response to humidity detection when there was no strain. We believe that with the advantages of high sensitivity, low cost, and high size controllability, the sensor has great application potential in minor strain and humidity detection. However, this CB/PVA sensor does not yet identify their respective contributions when strain and humidity vary simultaneously.

2. Design and Principle of Thin Film Sensor

2.1. The Design and Conductive Principle of the Sensor

The schematic diagram of the CB/PVA film sensor is shown in Figure 1a, which is composed of the CB/PVA composite film, a pair of metal electrodes (Cr/Au), and the Si/SiO₂ substrate. In principle, CB/PVA film can be used as both a strain sensor and humidity sensor. As shown in Figure 1b, working as a strain sensor, strain occurs in the CB/PVA film as the substrate deforms under pressure. It is important that the conductivity of the film decreases under pressure due to the displacement of carbon particles, resulting in discontinuous conducting channels in the film. Electrical studies were carried out to estimate the resistance values under strain or pressure. The change in magnitude of strain or pressure was obtained using the change in resistance values of the CB/PVA film. When used as a humidity sensor, the working mechanism of the CB/PVA film is shown in Figure 1c. Due to the hydrophilic hydroxyl group (–OH) in the molecule of PVA, the PVA-based film could adsorb the surrounding water molecules [24,26]. At low concentrations, the membrane adsorbed less water vapor, and the space between the CB particles was small enough to form more conductive channels and obtain smaller resistance. However, as the relative concentration increased, the CB/PVA polymer film swelled due to the adsorption of more water molecules, which enlarged the distance between carbon black particles and blocked the conductive channels [25,27]. Therefore, the electrical conductivity of the composite film decreased, and the resistance increased.

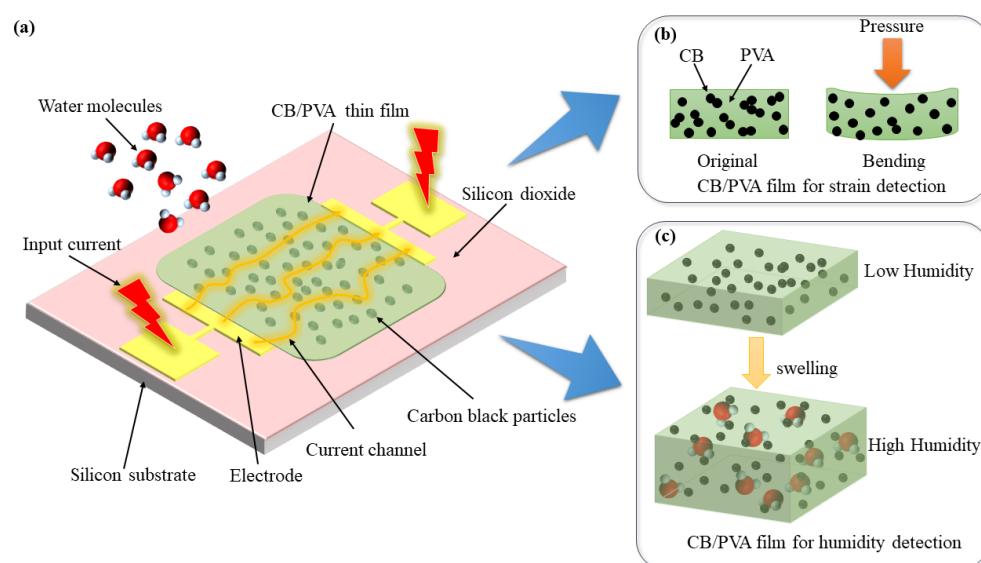


Figure 1. Structure and mechanism of CB/PVA film sensor. (a) Schematic diagram of CB/PVA film structure design. (b,c) Schematic diagram of the mechanism of CB/PVA film for strain detection (b) and humidity detection (c).

2.2. The Formation Mechanism of CB/PVA Film

Figure 2 illustrates the schematic diagram of the CB/PVA film formation mechanism using the droplet deposition method. It should be pointed out here that the deposition position of the droplet can be quickly and accurately controlled by the computer-controlled microscopic coating applicator. Due to the mutual attraction between the molecules, the CB/PVA droplet can be hemispherical at the tip of microscopic coating applicator's needle without falling, as seen in Figure 2a,d. In order to make the droplet contact with the droplet surface, the designed program can accurately control the tip of the micro coater to approach the surface of the silicon/silica substrate at a certain distance. When the droplet leaves the top surface of the substrate, one part of the droplet from the needle tip makes the surface of the substrate wet (that is, the droplet can form a plano-convex lens shape on the surface of the substrate), and the other part is left at the tip of the needle. Figure 2b shows that the diameter of each droplet is approximately 100 μm , which is determined by the diameter of the needle tip. Therefore, by changing the diameter of the needle tip, the droplet diameter can be controlled in the range of 50 μm to 200 μm . The distance between the center of the two droplets is nearly 80 μm when two droplets overlap each other. Due to the fluidity of the liquid, overlapping droplets will fuse with each other to form a new larger droplet. What is more, it has been reported that treating the composite film in an ethanol vapor atmosphere for 5 min can suppress the coffee ring effect and obtain a more uniform film. In future research, we will try this method to improve the uniformity of the film [38]. According to the designed route, the device moving in a straight line would align the droplets in several conductive film tapes, forming confined films with expected shapes after the overlapping of the droplets. In Figure 2c, the droplets are arranged in a 3×3 array, indicating that the microscopic coating applicator can precisely control the position of the droplets and the spacing between them to ensure better film formation uniformity. The thin films prepared using this method were ultra-thin and precisely controlled. Note that the thickness of CB/PVA films prepared by droplet deposition method ranged from a few nanometers to several hundreds of nanometers, depending on the resin concentration and the number of layers deposited. Undoubtedly, this method is suitable for not only preparing CB/PVA thin film but also for various polymer complex-based materials.

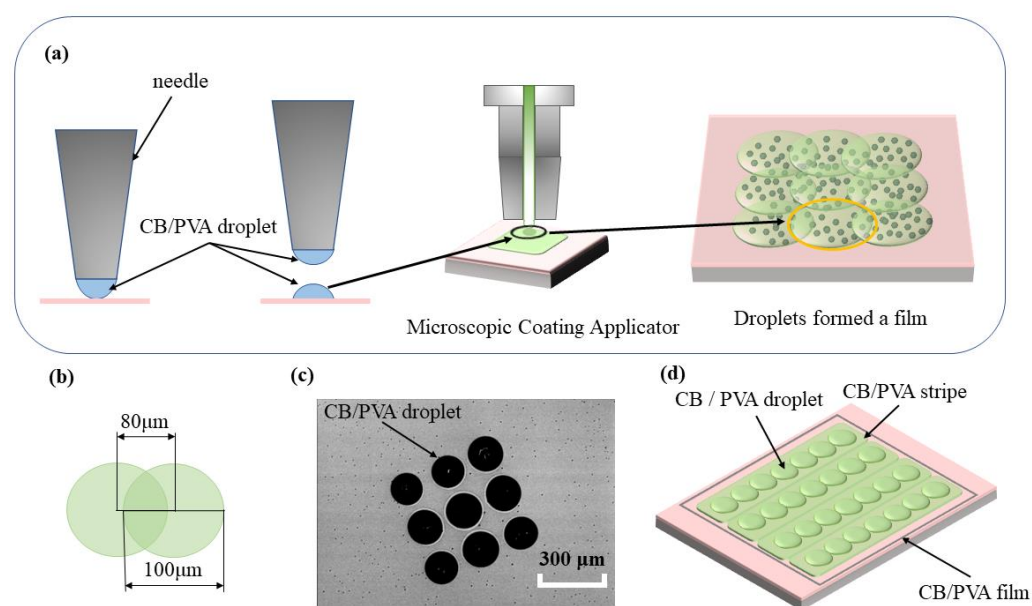


Figure 2. Schematic of film-forming mechanism of CB/PVA film. (a) Mechanism of droplets formation. (b) The distance between the centers of the droplets and the diameter of a droplet. (c) SEM image of deposited droplets. (d) The film formation by the droplet deposition method.

3. Experimental

3.1. CB/PVA Composite Film Fabrication Process

A step-by-step preparation process of the CB/PVA conductive polymer film is shown in Figure 3. First, a homogeneous PVA (the type of PVA was PVA 17-92, purchased from Sigma-Aldrich Co. Ltd., St. Louis, Missouri, USA) solution (6.25 wt%) was obtained by mixing the PVA crystals into 90 °C hot water and stirring constantly for ~30 min, as shown in Figure 3a,b. Then, the water-soluble carbon black (CB, from Lion Specialty Chemicals Co. Ltd., Tokyo, Japan; their mean particle diameter was 34 nm) dispersion (10 wt%) was added into the homogeneous PVA solution. In the mixed solution, the optimal content of carbon black was 2 wt%. In order to uniformly distribute the carbon black particles into the PVA polymer solution, the CB/PVA mixed dispersion was mixed in a planetary centrifugal mixer for 10 min (Figure 3c). To obtain solution homogeneity, the mixed solution was ultrasonicated for 60 min and further stirred for 10 min. The solution preparation was carried out at atmospheric conditions. However, to avoid unexpended film uniformity and residual stoichiometric variation from the air atmosphere, the film formation was handled at vacuum conditions. In particular, the mixed solution dispersion was placed in a vacuum drying oven for vacuum suction for ~60 min (Figure 3f). Then, the solution dispersion was moved into the microscopic coating applicator to form a thin film on a silicon/silicon dioxide substrate using the droplet deposition method (Figure 3g). Furthermore, CB/PVA films could also be deposited on glass or some flexible substrates such as polydimethylsiloxane. Finally, the film was cured in an oven at 80 °C for 30 min.

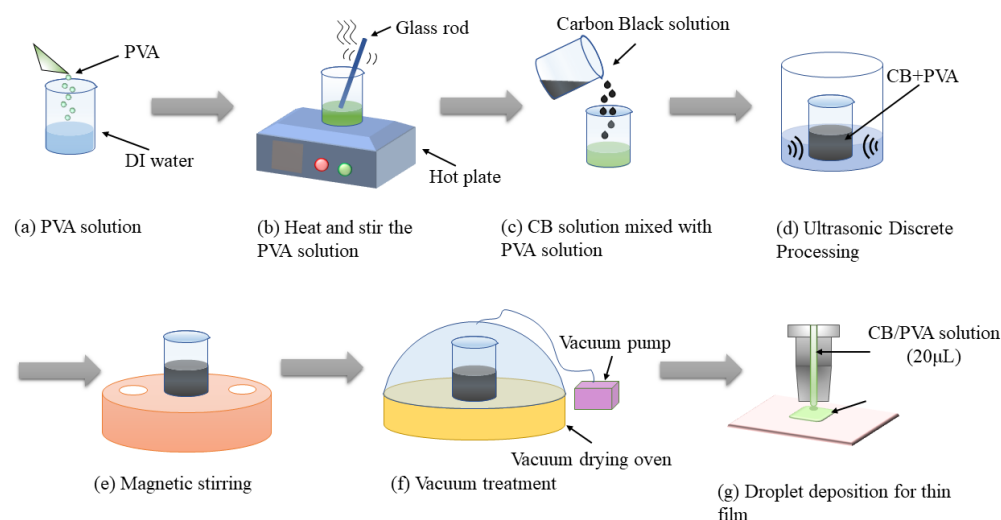


Figure 3. Schematic illustration of the preparation steps for the flexible CB/PVA film.

3.2. Four-Point Bending Method

In order to evaluate the electromechanical performance of the fabricated CB/PVA film as a strain sensor, we used the four-point bending method to obtain the GF value [39–42]. Figure 4 shows the schematic diagram of the four-point bending system to estimate the resistance change of the CB/PVA composite film under different loads. This system was composed of a computer, an I–V measurement unit, and a four-point bending device. The sensor substrate was 20 mm in length, 20 mm in width, and 300 µm in thickness. Note that the CB/PVA film was deposited in the center of the substrate. The sensor was placed on the measurement system, and the applied pressure was transmitted to the substrate through the four supports that generated small deformation of the substrate. In this work, the strain of the substrate and the film was very small, so it was difficult to measure and could not be calculated, and there was no slippage between them. However, the strain of

the CB/PVA film was the same as that of the substrate. Therefore, we could estimate the strain of the CB/PVA film by calculating the strain of the substrate using Formula (1).

$$\varepsilon = \frac{3Fa}{wt^2E} \quad (1)$$

where F is the sum of the force exerted on the upper support members, a is the shortest distance between the support and the outer support, w and t are the width and thickness, respectively, of the substrate, and E is the Young's modulus of the substrate material; the Young's modulus of the silicon/silicon dioxide substrate was about 185 GPa.

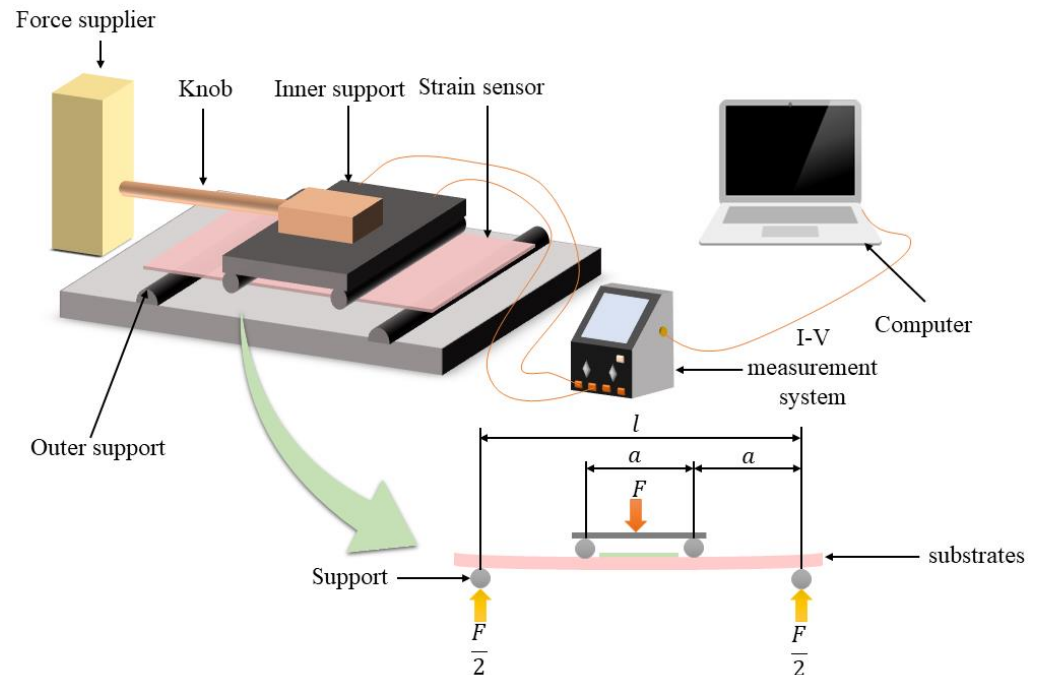


Figure 4. Schematic of the four-point bending method for testing the CB/PVA composite film strain sensor under different loads.

In traditional silicon-based strain devices, silicon materials are used as important pressure-sensitive elements in sensors. In addition, it is generally necessary to perform photolithography and other processes on silicon, which is a costly and complicated process [43–45]. However, in this work, the silicon/silicon dioxide base was only used as a strain-transmitting substrate material, and no additional processing was required for it. In addition, since it is not a sensitive component, it can also be replaced by other materials such as glass, PDMS, etc.

Obtaining the GF value of the sensor also requires knowledge of the change of the sensor resistance ($R = V/I$). The change in film resistance can be identified by the I–V measurement system, and the gauge factor of the strain sensor can be calculated by:

$$GF = \frac{\Delta R/R_0}{\Delta l/l_0} = \frac{\Delta R/R_0}{\varepsilon} \quad (2)$$

where $\Delta R = R - R_0$, is the changed resistance, and R_0 is the resistance value of the sensor when there is no strain [46,47].

4. Results and Discussion

Figure 5 shows the optical image of the fabricated strain and humidity sensing device. In order to observe the film formation phenomenon and the morphology of the sensor, as shown in Figure 5, we used transparent glass as the substrate for the morphology

observation. However, since silicon/silicon dioxide substrates are tougher than glass substrates, we used silicon/silicon dioxide as the sensor substrate when evaluating sensor performance. As seen in Figure 5, the electrodes were formed on the film by electron beam evaporation and photolithography. Initially, the Cr (20 nm) as an adhesion layer was deposited on the silicon/silicon dioxide substrate, and then the gold layer with a thickness of approximately 180 nm was deposited on the Cr layer as the electrode. Notably, the area of the fabricated electrode was $300 \times 300 \mu\text{m}$, where the CB/PVA film was majorly distributed, as seen in Figure 5b. What is more, by measuring with the segment differential gauge, we found that the thickness of the prepared film was only 400 nm. This result indicated that the prepared CB/PVA composite film was ultra-thin, which is one of the reasons for its high sensitivity under tiny strains.

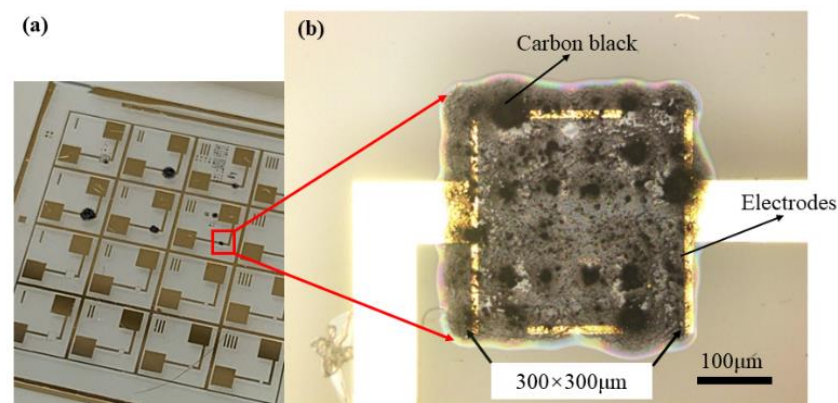


Figure 5. (a) Optical image of fabricated CB/PVA film sensor. (b) Micrograph of image of CB/PVA film.

In order to evaluate the resistance's stability of the fabricated CB/PVA film, the resistance of the samples was tested under different loads. The test voltage ranging from -5 V to 5 V was applied to the CB/PVA film. As seen in Figure 6a, it was observed that the current and voltage showed a linear relationship, which infers good contact between the electrode and the conductive film. This also indicates that the stability of the film resistance is excellent without any drift due to the applied strain. Moreover, the estimated resistance value of the film is $371.7 \text{ K}\Omega$ at a strain of 0.025% using the linear fit in the measured experimental data. In addition to examining the resistance stability of the sensor, we also examined the effects of strain and humidity on the CB/PVA film. For the purpose of avoiding the influence of various factors such as strain and humidity, we kept the humidity constant when detecting the strain sensitivity of the sensor. When detecting the effect of humidity on the resistance of the sensor, we ensured that the strain of the sensor was zero.

Figure 6b represents the change in resistance as a function of strain rate. The resistance of the sensor was $370.37 \text{ K}\Omega$ when the strain rate was zero. Under a constant load, force ranging from 0 N to 8 N with nine steps (the strain range of the substrate was $0\text{--}0.028\%$), the resistance value change of the CB/PVA film was measured using the four-point bending method (as shown in Figure 4). The final measurement result was the average of the three sets of measurement results. As can be seen in Figure 6b, there was almost a positive correlation between the resistance of the film and the applied strain. This indicates that under the increase in pressure, the conducting channels between the carbon black molecules may have been discontinuous due to the increases of the film strain. This resulted in a decrease in conductivity as the resistance of the film increased.

Figure 6c shows the relationship between the relative resistance variation of the sensor with various strain rates. It was found that the relative resistance increased with an increase in strain rate. Moreover, the increasing trend of the resistance change rate shown in Figure 6c was the same as that of the resistance change in Figure 6b.

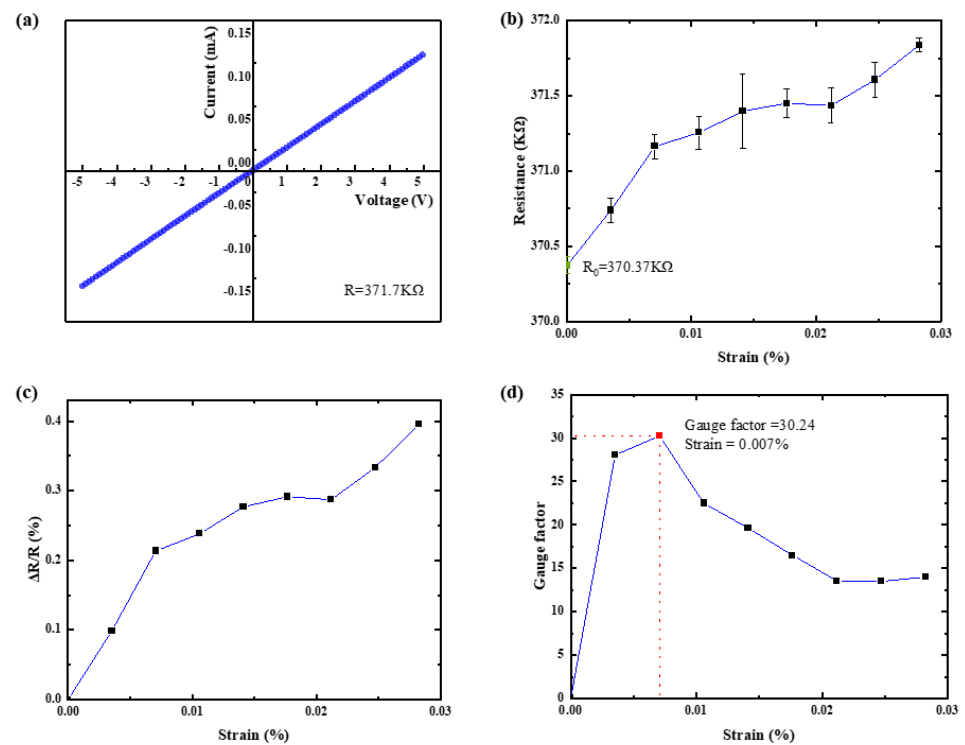


Figure 6. (a) I–V curve variation of CB/PVA composite with various loads evaluated using the four-point bending setup. (b) The change of film resistance under different strains. (c) The relative resistance change rates of the film under different strains. (d) The gauge factor of the CB/PVA film under different strains.

The gauge factor is a key parameter in analyzing the performance of strain sensors. It is defined as the change in resistance divided by the strain, which can be calculated using Equation (2). Figure 6d illustrates the estimated gauge factor of the CB/PVA film with various strain rates. As we can see, the highest gauge factor of the fabricated CB/PVA film sensor was about 30.24, which was measured when the strain was 0.007%. These results imply that the sensor has high sensitivity under low pressure and is expected to achieve ultra-sensitive detection such as pulse and vocal cord vibration detection.

The results presented in this work indicate excellent device characteristics using the CB/PVA thin films, which are comparable to the previously reported data (Table 1). Significantly, the CB/PVA film fabricated using the droplet deposition method had higher values of gauge factors under ultra-small strain. Furthermore, it was evident that the thin film had ultra-high sensitivity and could be applied to small pressure or strain.

Table 1. The previously reported GFs of strain sensors based on different sensitive materials or different film-forming methods are compared.

Material	Fabrication Methods	Gauge Factor	Reference
CB/PVA	Droplet deposition	30 at 0.007% strain	This work
CB/PVA	Spin coating	150	[40]
CB/PHOTONEECE	Spin coating	3.3	[40]
CB/AgNPs/TPU	Deposit via surface grafting	21.12 at 100% strain	[48]
PPy/PU	In situ polymerization	2.32 at 50% strain	[49]
SBS/CNT	Solution casting	120 at 20%	[39]
CB/ecoflex	Drop casting	1.62–3.37	[37]
CNT/NR	Knife coating	7.08 at 100%	[13]
CB/PVA	Screen Printing	10.68 at 3.21%	[50]
Graphene/cotton	Soaking	83.7 at 27%	[51]

As seen in Figure 7, the sensor was stabilized after being exposed to nitrogen for two minutes. Then, the relative humidity was maintained at 56.7%, 65.2%, and 73.7% for 2 min each by introducing water vapor, and the cycle was repeated three times. As a result, it is noteworthy that the reproducibility of the sensors under different humidity was very significant. As the humidity increased, the output voltage also increased correspondingly and responded more quickly.

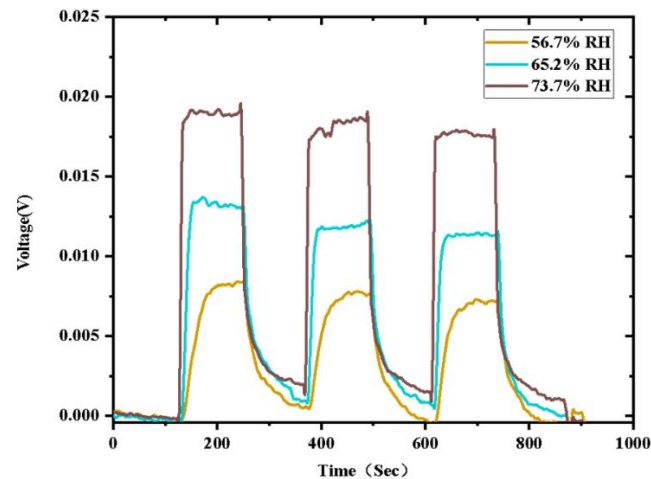


Figure 7. Repeated response of humidity sensor in different water vapor concentrations.

The response change of the sensor in different concentrations is shown in Figure 8. At room temperature, when the relative humidity was in the range of 10% to 70%, with increasing water vapor concentrations, the resistance value of the sensor also increased, which corresponds to the theoretical mechanism of the sensor. Note that the sensor had a relative resistance change rate of 0.8% at 10.9% RH. As can be seen from Figure 8, the sensor had good responses in different gradients of humidity. In addition, the sensor also exhibited enhanced sensing performance in terms of response and recovery times, which gradually decreased with increasing humidity.

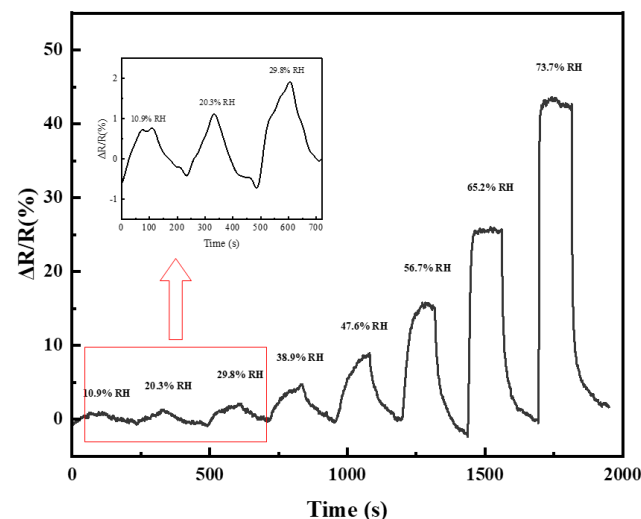


Figure 8. Response change of humidity sensor in different concentrations.

5. Conclusions

In conclusion, we demonstrated a CB/PVA conductive composite film sensor for micro-strain and humidity detection. The CB/PVA thin film prepared using the droplet deposition method reveals excellent device characteristics due to the ultra-thin thickness

and good sensitivity of the sensor. The film not only has a stable resistance under a constant strain, but it also has a gauge factor of 30 at a strain of 0.007%. What is more, the CB/PVA film sensor also showed good responses and repeatability in different concentrations of water vapor. These results contribute towards developing a CB/PVA-based composite thin-film minor strain and humidity sensor.

Author Contributions: Conceptualization, Z.W.; Data curation, Y.Z. and X.L.; Formal analysis, Y.Z., X.L. and Z.W.; Funding acquisition, Z.W.; Investigation, Y.Z. and Q.L.; Methodology, Z.W.; Supervision, X.L.; Validation, Z.W.; Visualization, Y.Z.; Writing—original draft, Y.Z.; Writing—review and editing, X.L. and X.W. All authors have read and agreed to the published version of the manuscript.

Funding: This research was funded by the project “Integrating Perception and Medical Detection Micro-Electromechanical Innovation” (Project Number: 0030904151004/016).

Institutional Review Board Statement: Not applicable.

Informed Consent Statement: Not applicable.

Data Availability Statement: Not applicable.

Conflicts of Interest: The authors declare no conflict of interest.

References

1. Kenry, Y.; Yeo, J.C.; Lim, C.T. Emerging flexible and wearable physical sensing platforms for healthcare and biomedical applications. *Microsyst. Nanoeng.* **2016**, *2*. [[CrossRef](#)]
2. Li, C.; Yang, S.; Guo, Y.; Huang, H.; Chen, H.; Zuo, X.; Fan, Z.; Liang, H.; Pan, L. Flexible, multi-functional sensor based on all-carbon sensing medium with low coupling for ultrahigh-performance strain, temperature and humidity sensing. *Chem. Eng. J.* **2021**, *426*, 130364. [[CrossRef](#)]
3. Weng, C.H.; Yang, Y.; Jia, J.; Liu, C.; Mao, D.; Weerasinghe, R.; Wu, J. Decoupling and decomposition analysis on the CO₂ emissions of tourism industry: A case study of Hainan. *E3S Web Conf.* **2019**, *118*, 04042. [[CrossRef](#)]
4. Hossain, M.M.; Toda, M.; Hokama, T.; Yamazaki, M.; Moorthi, K.; Ono, T. Piezoresistive Nanomechanical Humidity Sensors Using Internal Stress In-Plane of Si-Polymer Composite Membranes. *IEEE Sens. Lett.* **2019**, *3*, 2500404. [[CrossRef](#)]
5. Zhang, L.; Wang, Y.; Wei, Y.; Xu, W.; Fang, D.; Zhai, L.; Lin, K.-C.; An, L. A Silicon Carbonitride Ceramic with Anomalously High Piezoresistivity. *J. Am. Ceram. Soc.* **2008**, *91*, 1346–1349. [[CrossRef](#)]
6. Ruhhammer, J.; Zens, M.; Goldschmidtboeing, F.; Seifert, A.; Woias, P. Highly elastic conductive polymeric MEMS. *Sci. Technol. Adv. Mater.* **2015**, *16*, 015003. [[CrossRef](#)] [[PubMed](#)]
7. Mannsfeld, S.C.; Tee, B.C.; Stoltenberg, R.M.; Chen, C.V.; Barman, S.; Muir, B.V.; Sokolov, A.N.; Reese, C.; Bao, Z. Highly sensitive flexible pressure sensors with microstructured rubber dielectric layers. *Nat. Mater.* **2010**, *9*, 859–864. [[CrossRef](#)] [[PubMed](#)]
8. Latessa, G.; Brunetti, F.; Reale, A.; Saggio, G.; Di Carlo, A. Piezoresistive behaviour of flexible PEDOT:PSS based sensors. *Sens. Actuators B Chem.* **2009**, *139*, 304–309. [[CrossRef](#)]
9. Wang, C.; Xia, K.; Wang, H.; Liang, X.; Yin, Z.; Zhang, Y. Advanced Carbon for Flexible and Wearable Electronics. *Adv. Mater.* **2019**, *31*, e1801072. [[CrossRef](#)] [[PubMed](#)]
10. Nag, A.; Mitra, A.; Mukhopadhyay, S.C. Graphene and its sensor-based applications: A review. *Sens. Actuators A Phys.* **2018**, *270*, 177–194. [[CrossRef](#)]
11. Novoselov, K.S.; Fal’ko, V.I.; Colombo, L.; Gellert, P.R.; Schwab, M.G.; Kim, K. A roadmap for graphene. *Nature* **2012**, *490*, 192–200. [[CrossRef](#)]
12. Lee, S.; Reuveny, A.; Reeder, J.; Lee, S.; Jin, H.; Liu, Q.; Yokota, T.; Sekitani, T.; Isoyama, T.; Abe, Y.; et al. A transparent bending-insensitive pressure sensor. *Nat. Nanotechnol.* **2016**, *11*, 472–478. [[CrossRef](#)]
13. Tran, L.; Kim, J. A Comparative Study of the Thermoplastic Polyurethane/Carbon Nanotube and Natural Rubber/Carbon Nanotube Composites According to Their Mechanical and Electrical Properties. *Fibers Polym.* **2018**, *19*, 1948–1955. [[CrossRef](#)]
14. Stampfer, C.; Jungen, A.; Linderman, R.; Obergefell, D.; Roth, S.; Hierold, C. Nano-electromechanical displacement sensing based on single-walled carbon nanotubes. *Nano Lett.* **2006**, *6*, 1449–1453. [[CrossRef](#)] [[PubMed](#)]
15. Amjadi, M.; Yoon, Y.J.; Park, I. Ultra-stretchable and skin-mountable strain sensors using carbon nanotubes-Ecoflex nanocomposites. *Nanotechnology* **2015**, *26*, 375501. [[CrossRef](#)] [[PubMed](#)]
16. Zhu, S.-E.; Krishna Ghatkesar, M.; Zhang, C.; Janssen, G.C.A.M. Graphene based piezoresistive pressure sensor. *Appl. Phys. Lett.* **2013**, *102*, 161904. [[CrossRef](#)]
17. Tian, H.; Shu, Y.; Wang, X.F.; Mohammad, M.A.; Bie, Z.; Xie, Q.Y.; Li, C.; Mi, W.T.; Yang, Y.; Ren, T.L. A graphene-based resistive pressure sensor with record-high sensitivity in a wide pressure range. *Sci. Rep.* **2015**, *5*, 8603. [[CrossRef](#)]
18. Watthanawisuth, N.; Matusros, T.; Sappat, A.; Tuantranont, A.; Ieee. The IoT Wearable Stretch Sensor Using 3D-Graphene Foam. In *2015 IEEE Sensors*; IEEE: New York, NY, USA, 2015; pp. 426–429.

19. An, Z.; Li, J.; Kikuchi, A.; Wang, Z.; Jiang, Y.; Ono, T. Mechanically strengthened graphene-Cu composite with reduced thermal expansion towards interconnect applications. *Microsyst. Nanoeng.* **2019**, *5*, 20. [[CrossRef](#)] [[PubMed](#)]
20. Li, X.; Zhang, R.; Yu, W.; Wang, K.; Wei, J.; Wu, D.; Cao, A.; Li, Z.; Cheng, Y.; Zheng, Q.; et al. Stretchable and highly sensitive graphene-on-polymer strain sensors. *Sci. Rep.* **2012**, *2*, 870. [[CrossRef](#)]
21. Huang, J.-C. Carbon black filled conducting polymers and polymer blends. *Adv. Polym. Technol.* **2002**, *21*, 299–313. [[CrossRef](#)]
22. Xiao, H.; Li, H.; Ou, J. Modeling of piezoresistivity of carbon black filled cement-based composites under multi-axial strain. *Sens. Actuators A Phys.* **2010**, *160*, 87–93. [[CrossRef](#)]
23. Nan, N.; DeVallance, D.B. Development of poly(vinyl alcohol)/wood-derived biochar composites for use in pressure sensor applications. *J. Mater. Sci.* **2017**, *52*, 8247–8257. [[CrossRef](#)]
24. Das, M.; Sarkar, D. Development of room temperature ethanol sensor from polypyrrole (PPy) embedded in polyvinyl alcohol (PVA) matrix. *Polym. Bull.* **2017**, *75*, 3109–3125. [[CrossRef](#)]
25. Jiang, K.; Fei, T.; Jiang, F.; Wang, G.; Zhang, T. A dew sensor based on modified carbon black and polyvinyl alcohol composites. *Sens. Actuator B-Chem.* **2014**, *192*, 658–663. [[CrossRef](#)]
26. Krishna, A.; Kumar, A.; Singh, R.K. Effect of Polyvinyl Alcohol on the Growth, Structure, Morphology, and Electrical Conductivity of Polypyrrole Nanoparticles Synthesized via Microemulsion Polymerization. *ISRN Nanomater.* **2012**, *2012*, 809063. [[CrossRef](#)]
27. Maity, D.; Rajavel, K.; Kumar, R.T.R. Polyvinyl alcohol wrapped multiwall carbon nanotube (MWCNTs) network on fabrics for wearable room temperature ethanol sensor. *Sens. Actuators B Chem.* **2018**, *261*, 297–306. [[CrossRef](#)]
28. Mbam, S.O.; Nwonu, S.E.; Orelaja, O.A.; Nwigwe, U.S.; Gou, X.-F. Thin-film coating; historical evolution, conventional deposition technologies, stress-state micro/nano-level measurement/models and prospects projection: A critical review. *Mater. Res. Express* **2019**, *6*, 122001. [[CrossRef](#)]
29. Zhang, S.; Li, S.; Xia, Z.; Cai, K. A review of electronic skin: Soft electronics and sensors for human health. *J. Mater. Chem. B* **2020**, *8*, 852–862. [[CrossRef](#)]
30. Krebs, F.C. Fabrication and processing of polymer solar cells: A review of printing and coating techniques. *Sol. Energy Mater. Sol. Cells* **2009**, *93*, 394–412. [[CrossRef](#)]
31. Zhou, X.; Zhu, L.; Fan, L.; Deng, H.; Fu, Q. Fabrication of Highly Stretchable, Washable, Wearable, Water-Repellent Strain Sensors with Multi-Stimuli Sensing Ability. *ACS Appl. Mater. Interfaces* **2018**, *10*, 31655–31663. [[CrossRef](#)]
32. Qi, X.; Li, X.L.; Jo, H.; Bhat, K.S.; Kim, S.; An, J.; Kang, J.W.; Lim, S. Mulberry paper-based graphene strain sensor for wearable electronics with high mechanical strength. *Sens. Actuator A-Phys.* **2020**, *301*, 8. [[CrossRef](#)]
33. Yu, Z.; Zhang, Q.; Li, L.; Chen, Q.; Niu, X.; Liu, J.; Pei, Q. Highly flexible silver nanowire electrodes for shape-memory polymer light-emitting diodes. *Adv. Mater.* **2011**, *23*, 664–668. [[CrossRef](#)] [[PubMed](#)]
34. Kim, J.H.; Kim, S.R.; Kil, H.J.; Kim, Y.C.; Park, J.W. Highly Conformable, Transparent Electrodes for Epidermal Electronics. *Nano Lett.* **2018**, *18*, 4531–4540. [[CrossRef](#)]
35. Ke, K.; McMaster, M.; Christopherson, W.; Singer, K.D.; Manas-Zloczower, I. Highly sensitive capacitive pressure sensors based on elastomer composites with carbon filler hybrids. *Compos. Part A Appl. Sci. Manuf.* **2019**, *126*, 105614. [[CrossRef](#)]
36. Liu, H.; Jiang, H.; Du, F.; Zhang, D.; Li, Z.; Zhou, H. Flexible and Degradable Paper-Based Strain Sensor with Low Cost. *ACS Sustain. Chem. Eng.* **2017**, *5*, 10538–10543. [[CrossRef](#)]
37. Shintake, J.; Piskarev, Y.; Jeong, S.H.; Floreano, D. Ultrasstretchable Strain Sensors Using Carbon Black-Filled Elastomer Composites and Comparison of Capacitive Versus Resistive Sensors. *Adv. Mater. Technol.* **2017**, *3*, 1700284. [[CrossRef](#)]
38. Guo, Y.; Ono, Y.; Nagao, Y. Modification for Uniform Surface of Nafion Ultrathin Film Deposited by Inkjet Printing. *Langmuir* **2015**, *31*, 10137–10144. [[CrossRef](#)]
39. Costa, P.; Ferreira, A.; Sencadas, V.; Viana, J.C.; Lanceros-Méndez, S. Electro-mechanical properties of triblock copolymer styrene-butadiene-styrene/carbon nanotube composites for large deformation sensor applications. *Sens. Actuators A Phys.* **2013**, *201*, 458–467. [[CrossRef](#)]
40. Huang, Y.-T.; Inomata, N.; Wang, Z.; Lin, Y.-C.; Ono, T. Flexible Porous Carbon Black-Polymer Composites with a High Gauge Factor. *Sens. Mater.* **2020**, *32*, 2527–2538. [[CrossRef](#)]
41. Zhu, M.; Sakamoto, K.; Li, J.; Inomata, N.; Toda, M.; Ono, T. Piezoresistive strain sensor based on monolayer molybdenum disulfide continuous film deposited by chemical vapor deposition. *J. Micromech. Microeng.* **2019**, *29*, 055002. [[CrossRef](#)]
42. Zhu, M.; Li, J.; Inomata, N.; Toda, M.; Ono, T. Vanadium-doped molybdenum disulfide film-based strain sensors with high gauge factor. *Appl. Phys. Express* **2019**, *12*, 015003. [[CrossRef](#)]
43. Salvatori, S.; Pettinato, S.; Piccardi, A.; Sedov, V.; Voronin, A.; Ralchenko, V. Thin Diamond Film on Silicon Substrates for Pressure Sensor Fabrication. *Materials* **2020**, *13*, 3697. [[CrossRef](#)] [[PubMed](#)]
44. Pedersen, T.; Fragiaco, G.; Hansen, O.; Thomsen, E.V. Highly sensitive micromachined capacitive pressure sensor with reduced hysteresis and low parasitic capacitance. *Sens. Actuators A Phys.* **2009**, *154*, 35–41. [[CrossRef](#)]
45. Bae, B.; Flachsbar, B.R.; Park, K.; Shannon, M.A. Design optimization of a piezoresistive pressure sensor considering the output signal-to-noise ratio. *J. Micromech. Microeng.* **2004**, *14*, 1597–1607. [[CrossRef](#)]
46. Barlian, A.A.; Park, W.T.; Mallon, J.R., Jr.; Rastegar, A.J.; Pruitt, B.L. Review: Semiconductor Piezoresistance for Microsystems. *Proc. IEEE Inst. Electr. Electron. Eng.* **2009**, *97*, 513–552. [[CrossRef](#)] [[PubMed](#)]
47. Fiorillo, A.S.; Critello, C.D.; Pullano, S.A. Theory, technology and applications of piezoresistive sensors: A review. *Sens. Actuators A Phys.* **2018**, *281*, 156–175. [[CrossRef](#)]

48. Zhang, W.; Liu, Q.; Chen, P. Flexible Strain Sensor Based on Carbon Black/Silver Nanoparticles Composite for Human Motion Detection. *Materials* **2018**, *11*, 1836. [[CrossRef](#)]
49. Li, M.; Li, H.; Zhong, W.; Zhao, Q.; Wang, D. Stretchable conductive polypyrrole/polyurethane (PPy/PU) strain sensor with netlike microcracks for human breath detection. *ACS Appl. Mater. Interfaces* **2014**, *6*, 1313–1319. [[CrossRef](#)]
50. Sekertekin, Y.; Bozyel, I.; Gokcen, D. A Flexible and Low-Cost Tactile Sensor Produced by Screen Printing of Carbon Black/PVA Composite on Cellulose Paper. *Sensors* **2020**, *20*, 2908. [[CrossRef](#)] [[PubMed](#)]
51. Li, K.; Yang, W.; Yi, M.; Shen, Z. Graphene-based pressure sensor and strain sensor for detecting human activities. *Smart Mater. Struct.* **2021**, *30*, 085027. [[CrossRef](#)]